Gated, Ion-selective Channels Observed with Patch Pipettes in the Absence of Membranes: Novel Properties of a Gigaseal

Frederick Sachs and Feng Qin
MRC Hills Road, Cambridge CB2 2QH, England, and Biophysics, State University of New York, Buffalo, New York 14124 USA

ABSTRACT Gigaohm seals made between patch pipettes and hydrophobic substrates have a finite conductance which are cation-selective and capable of producing quantized gating indistinguishable from the gating of biological ion channels. The selectivity sequence and streaming potentials of these seals suggests the existence of a pore of similar dimensions to the nicotinic acetylcholine channel. The ionic selectivity of these seals appears similar to the seal selectivity observed with membrane patches (Fischmeister, R., R. K. Ayer, and R. L. DeHann. 1986. *Pfluegers Arch.* 406:73–82) and the possibility of discrete gating within the seal region suggests caution when interpreting patch clamp data from unfamiliar preparations. The data suggests that the permeation pathway is the narrow space between the hydrophobic substrate and the pipette. Since this space has one hydrophobic wall, a hydrophilic channel lining may not be essential for channel permeation and gating.

INTRODUCTION

While performing control experiments that involved sealing patch pipettes against a surface made of Sylgard, a hydrophobic silicone rubber, we noticed currents that appeared identical to those seen with ion channels in patch-clamped membranes. Rather amazed, we looked more closely at the permeation and gating properties of these "rubber channels" and found that they mimicked many aspects of membrane-bound channels. The seals were perm-selective for small cations and had a permeation pathway of molecular dimensions. The gating of the seal exhibited binary gating, mode shifting, and voltage-dependent kinetics.

Little is known about the properties of gigaohm seals on membranes, since the measurement of seal resistance requires that the potential across the seal and the membrane be independently controlled. In the only published study of this kind, Fischmeister et al. (1986) found that under bi-ionic conditions with the pipette containing $CaCl_2$ and the bath containing NaCl, the seal resistance was voltage-dependent and selective for Na^+ over Ca^{2+}. The seals we have studied here have similar properties, and the similarity suggests caution in interpreting patch clamp data, particularly from new preparations. These seals may be a useful model system for studying ion activity in small spaces, since the selectivity can be varied by the force between the pipette and the substrate, the surfaces can be chemically modified, nonaqueous solvents can be used, and the voltage range is virtually unlimited.

MATERIALS AND METHODS

Patch pipettes were pulled from thick and thin wall (1-mm OD, 0.7- and 0.5-mm ID) wall borosilicate, alumino silicate, and quartz capillaries (Clark Electromedical, Pangbourne, Reading, UK) on a Sutter PC-2000 puller (Sutter Instrument Co., Novato, CA). Tip sizes ranged from an OD of about 1 μm to 0.1 mm. The borosilicate tips had nearly parallel walls, while the quartz tips had a steeper taper of about 10°. The pipettes were sometimes silanized to create a hydrophobic surface by dipping the tips into dimethyldichlorosilane dissolved in tricloroethane (BDH Ltd., Poole, England) after filling the pipette with saline. To provide low drift, pipettes were clamped to a glass rod held at about 10° from the horizontal in a piezoelectric micromanipulator (PZS-1000; Burleigh Instruments, Fishers, NY). Movement of the pipette tip was calibrated using the manipulator's conversion factor of 0.7 μm/V. Currents were recorded with an Axopatch 1D amplifier (Axon Instruments, Foster City, CA), and single channel data were stored on a DTR-1202 digital tape recorder (Instruments de Laboratories, Claix, France). Single channel data was digitized with an Axon Instruments TL-1 DMA interface driven by PCLAMP software (Axon Instruments) on a personal computer. Current/voltage (I/V) data were collected with ramp protocols using PCLAMP. The pipette electrode was a chlorided silver wire and the bath electrode was a patch pipette filled with 3 M KCl connected to a chlorided silver wire. The pipette position was observed with a Zeiss Axiovert microscope using DIC optics with a 63 × planapo oil immersion objective and a condenser consisting of a 40 × water immersion objective illuminated by a 50-watt mercury arc through a fiber optic scrambler.

Hydrophobic insulating surfaces were prepared from Sylgard 184 (Dow Corning) using manufacturer's guidelines: by weight, 1:10, catalyst:resin. Sylgard was well mixed, degassed in a vacuum, then spread thinly over a number 1 coverslip using a Gilson yellow tip pipette as a spreader. The coverslips were placed on a 50°C hotplate for about 20 min to cure. Then a thin ring of Sylgard was added to form a shallow chamber, and this was cured as before. One series was done with a thin layer of Vaseline (Cheesborough Ponds) on the coverslips and another with small pieces of Saran Wrap (Dow Corning) stuck to the coverslip by heating at 50°C.

Stock solutions of test cations consisted of 400 mM chloride salts buffered with 5 mM 4-morpholinepropanesulfonic acid (MOPS; neutralized with NaOH) with the exception of HCl and NaOH which were unbuffered. To vary concentration, these stocks were diluted appropriately with water.

Prior to making a recording, the voltage offset was carefully adjusted to produce zero current. The pipette was lowered to the surface, and when the resistance increased to about 100 MΩ, we recorded the resistance (R_o), the short circuit current (I_o), and the open circuit voltage (reversal potential, V_r) as a function of insertion depth. The seal resistance was measured using a 20-mV square wave and sometimes checked as the ratio of reversal potential to short circuit current. Voltages always refer to the pipette potential relative to the bath. The input current of the amplifier was 0.12 pA as measured by integration on a known capacitance. During current clamp measurements the observed voltages should be accurate to $\cong$1 mV for seals <10 GΩ and to $\cong$10 mV for seals < 100 GΩ. We didn't include any voltage measurement whose magnitude was comparable to these values. We measured the liquid junction potential (ljp) across the pipette/solution interface with a patch pipette filled with the reference solution and a bath electrode of 3 M KCl. To begin, the bath was filled with the reference solution, and the clamp

Received for publication 31 August 1992 and in final form 12 May 1993.

0006-3495/93/09/1101/07 $2.00

output was set to zero. The ljp values were then measured in current clamp by changing the bath solution from the reference solution to the test solution using three separate washes of the test solution. For dilution potentials, the ljp values were always measured with increasing concentrations of bath solution to minimize the effects of contamination. Relative to 400 mM NaCl, the ljp values of the Cl salts of 400 mM monovalents, 200 mM divalents, and 133 mM trivalents were (in millivolts): H 29.3, Cs 4, Rb 4,K 3, guanidine 0, Li −1, ACh −2.8, Tris −3.7, Arg −4.8, Ca −15.5, Mg −16.2, Sr −18.3, Ba −18.5, Mn −20. For dilution potentials, (pipette:bath, 10:1), the ljp values were: H −36.2, Cs −0.7, Rb −1, K −0.3, guanidine 10.3, Li 16, ACh 15.5, Tris 28, Arg 18.5, Ca 17, Mg 13.3, Sr 19.3, Ba 19.5, Mn 23. For monovalent salts, the ljp values were close to those predicted by the Planck-Henderson equation, but for the higher valences we found significant discrepancies and always used the measured value. Permeability ratios for seals were calculated from bi-ionic and dilution data using the Goldman-Hodgkin-Katz voltage equation (Hille, 1984) including P_{Cl^-}.

RESULTS

We observed discrete gating with approximately 30% of the pipettes in a variety of solutions. Most of the activity was observed with seals of intermediate resistance, 2–10 GΩ, but sometimes with resistances of >100 GΩ. Fig. 1 *A* shows an example of persistent (Fig. 1 *B*) binary activity. It should be noted that the low conductance, "closed," state still carried a substantial current. The kinetics were not stationary for long periods, so we did not attempt a quantitative analysis, but duration histograms of data such as that shown in Fig. 1 *A* could be well fit with one or two exponential components (data not shown). We usually saw different gating modes. Fig. 1 *C* shows an example in which there was a modal change in both amplitude and kinetics. These kind of data emphasize that it is possible to obtain data from a single gated pathway since there was no overlap of the different modes.

Discrete gating (as opposed to unresolved fluctuations) was observed mainly with borosilicate glass and on one occasion with a quartz pipette. Quartz tended to form seals >100 GΩ with displacements of 0.1–0.2 μm into the surface, making it difficult to study. This rapid sealing may be a result of the fact that quartz is less hydrophilic than glass and more easily dehydrated. Discrete gating could be abolished by increasing or decreasing the force on the pipette, but the changes in gating associated with changes in depth were not consistent or easily characterized. For loose seals, the noise level increased significantly with the current but for tight seals, it was less pronounced. The current noise of a given conductance state always decreased with increasing seal resistance.

Fig. 2 demonstrates the process of forming seals against Sylgard for borosilicate and quartz pipettes. The pipettes contained 3 M KCl, and the bath contained 1.5 mM KCl. They were positioned about 1 μm above the Sylgard surface, the background currents were balanced to near zero, and then the manipulator was commanded to ramp 2 μm toward the surface. As the pipettes touched the surface, the sealing region became cation-selective creating a diffusion potential. This potential drove a current $I(x) = V(x)g(x)$ through the

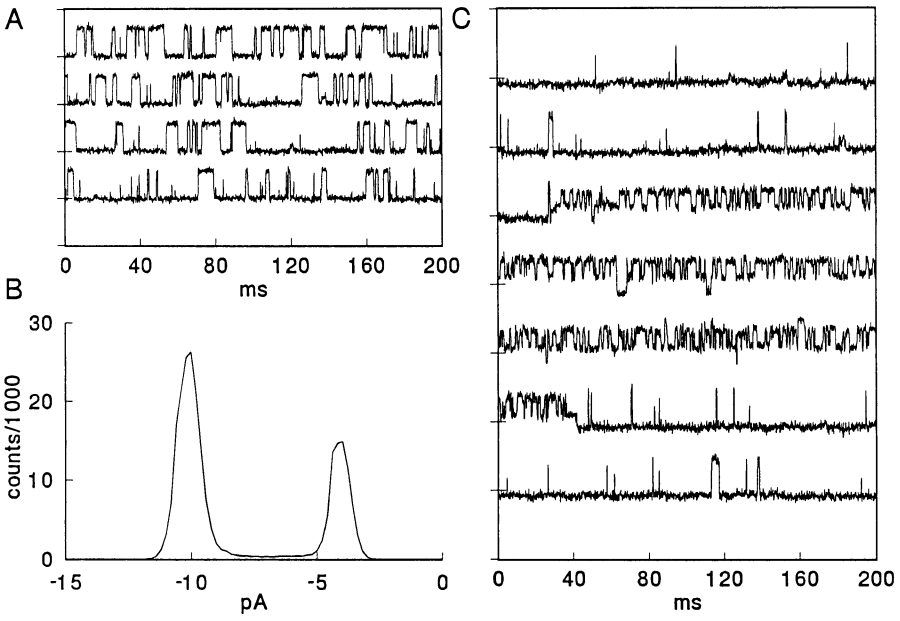

FIGURE 1 (*A*) Selected single channel data showing binary gating. The tick marks are at 10-pA intervals, and the baseline for each trace is at the tick mark one division *above* each trace, i.e., the baseline for the upper trace is the upper border of the panel. The low conductance state has about 25% the conductance of the high conductance state. The pipette contained 360 mM NaCl plus 40 mM NaF (Note: fluoride is present but not necessary to see channel behavior). The bath contained 400 mM NaCl. Pipette potential −300 mV, bandwidth 5 kHz, sampled at 50 μs/pt. (*B*) Amplitude histogram of the data from *A* showing maintained binary behavior for 12 s. (*C*) Multiple modes of gating. Conditions and display as in *A* but pipette potential −200 mV. At the beginning of the plot, the channel was open nearly all the time. In trace three, the conductance dropped so that the high conductance state was about half of its earlier amplitude, while the low conductance state had about the same amplitude. Simultaneously, the kinetics became faster and shifted closer to a 50% duty cycle. A few full size openings were mixed in with the subconductance states. After several seconds, the old kinetics resumed. The data is continuous from top to bottom with the exception of a three second gap between traces 4 and 5 during which the activity was similar to that shown in the contiguous segments.

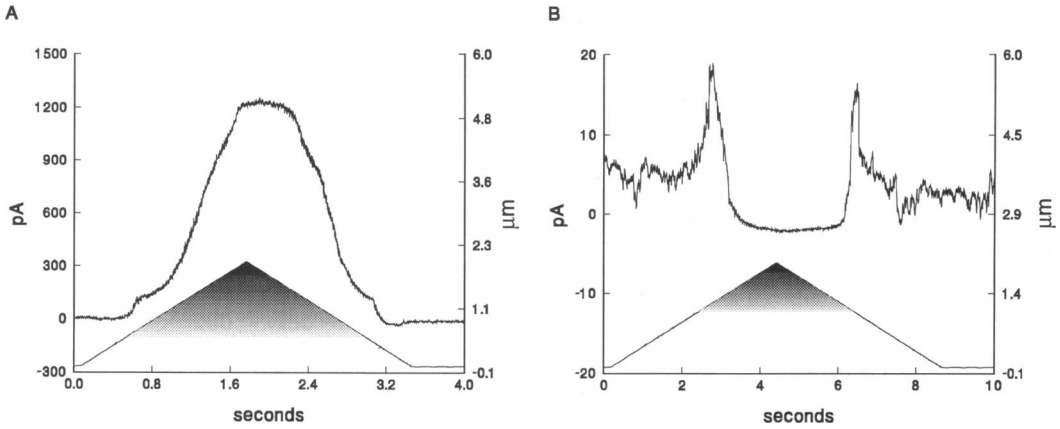

FIGURE 2 Short circuit current as a function of depth of insertion into Sylgard. (*A*) Borosilicate glass; (*B*) quartz. The pipettes contained 3 M KCl and the bath contained 1.5 mM KCl. The pipette position is shown in the lower traces (*right-hand axis*), with shading indicating the portion of the scan during which the pipette was in contact with Sylgard. As the pipettes touched the surface, the sealing region became cation selective creating a large diffusion potential driving current through the seal resistance. In the case of borosilicate glass (*A*), the driving force increased faster than the seal resistance so that the current was a monotonic function of depth. For quartz pipettes (*B*), the seal was also cation selective, but the seal resistance increased so rapidly with depth that the current returned to zero within a few tenths of a micron. Gated currents were observed with the pipette in (A). Some activity can be seen as noise in the maximum depth region of this low gain recording pipette resistances: *A*, 200 MΩ; *B*, 3 MΩ.

seal resistance, where x is the distance into Sylgard, $V(x)$ is the driving force, and $g(x)$ is the conductance of the seal. In the case of borosilicate glass (Fig. 2 *A*), the driving force increased faster than the seal resistance so that the current was a monotonic function of depth. For quartz pipettes (Fig. 2 *B*), the seal was cation selective, but the seal resistance increased so rapidly with depth that, after the initial increase, the current fell to zero within a few tenths of a micron. Silane-treated pipettes varied between the behavior in *A* and *B*.

To characterize the permeation pathway, we first examined the cation/anion selectivity of the seals. Unless otherwise stated, in what follows we refer only to seals that did not show discrete gating. With a 10-fold concentration gradient between the patch pipette and the bath, we measured the reversal potential as a function of insertion depth. Increasing depth increased the seal resistance, the open circuit voltage, the selectivity for cations over anions and decreased the short circuit current (Fig. 3 *A*).

The preference for small cations over anions was consistent for all the pipette glasses tested (borosilicate, aluminosilicate, and quartz) and all the hydrophobic surfaces tested (Sylgard, Vaseline, and Saran), but we only characterized the borosilicate/Sylgard interface in detail. The permeability ratio, P_X/P_{Cl}, calculated from the GHK (Goldman-Hodgkin-Katz) voltage equation (Hille, 1984) generally followed the aqueous mobility but with significant deviations, most notably H^+ (Table 1).

From reversal potentials, the cation selectivity referred to Cl^- was

$$Na^+ > K^+ > Cs^+ > Rb^+ > Li^+ > Guan^+ > H^+ > Mg^{2+} > Sr^{2+} > Ca^{2+} > Tris^+ > Ba^{2+} > Mn^{2+} > Arg^+ > La^{3+} > ACh^+.$$

As expected from the role of image forces on partitioning of ions into a low dielectric medium (Hille, 1984), the permeability decreased roughly as the square of the valence. The reversal potentials varied somewhat with different pipettes, even when the depth of insertion was held constant. Repeated seals with the same pipette had similar properties. The variability indicated by the standard errors in Table 1 is dominated by the variance between pipettes. Because small changes in the potentials could alter the order of adjacent entries in Table 1, the permeability sequence above is only approximate.

To obtain a more direct measure of cation selectivity we measured bi-ionic potentials referred to Na^+ with Cl^- as the common anion. As with the dilution potentials, the selectivity increased with insertion depth (Fig. 3 *B*). The selectivity sequence generally followed the trend expected from dilution potentials (Table 1), but the average sequence,

$$H^+ > Cs^+ > Rb^+ > K^+ > Guan^+ > Na^+ > Li^+ > Arg^+ > Ca^{2+} > Ba^{2+} > Sr^{2+} > Mn^{2+} > Tris^+ > Mg^{2+},$$

was much closer to that of the aqueous mobility. The large bi-ionic potentials seen with the less permeant cations referred to Na^+ were variable, so we also made measurements using Mg^{2+} and $Tris^+$ as reference ions (Table 2). These produced some inversions but, consistently, the monovalent alkali ions were more permeant than the divalents or the large organic ions. The bi-ionic sequence relative to Na^+ is similar to that of the nicotinic receptor/channel and suggests a large, low field, aqueous pore (Adams et al., 1980; Dwyer et al., 1980; Adams et al., 1981; Hille, 1984).

We examined the anion permeation properties relative to Cl^- under bi-ionic conditions with Na^+ as the common cation. From reversal potentials, the permeability sequence was: $F^- > Acetate^- > Cl^- > I^- > OH^-$, the inverse of the free

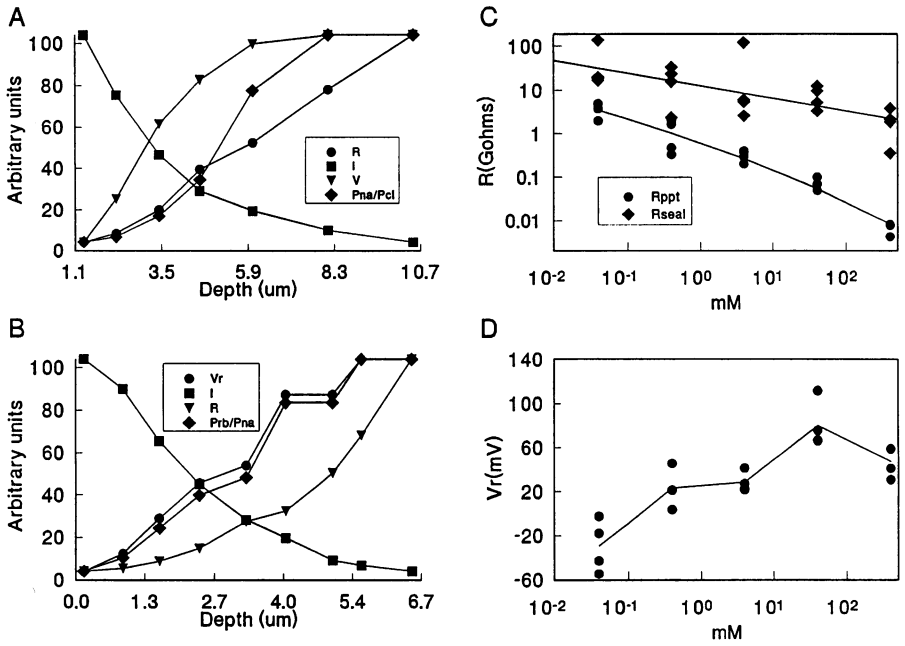

FIGURE 3 (*A*) The variation with depth of insertion of short circuit current (I), open circuit voltage (V), pipette resistance (R), and cation/anion selectivity (P_{Na^+}/P_{Cl^-}) of a seal between a borosilicate pipette and a Sylgard surface. The pipette contained 400 mM NaCl and the bath 40 mM NaCl. All data has been scaled to 100. For each trace the minimum/maximum are: I (26/181 pA); V (−4.1/−51.1 mV); R (.07/2.2 GΩ); P_{Na^+}/P_{Cl^-} (1.2/30.6). (*B*) The increase of cationic selectivity with depth. The pipette contained 400 mM NaCl and the bath 400 mM RbCl. The data was labeled and scaled as in *A*. Minimum/maximum: I (−42.5/−3.5 pA); V (29/41 mV); R (0.67/10 GΩ); P_{Rb^+}/P_{Na^+} (3.3/5.4). (*C*) The variation with concentration of pipette resistance (R_{ppt}) and seal resistance (R_{seal}) under bi-ionic conditions (LiCl in bath, KCl in the pipette). The R_{seal} has been fit to a model (regression line) with a volume conductance and a surface conductance in parallel: $R_{ppt}^{-1} = C(A - BC^{1/2}) + EC^{1/2}$ with $A = 0.25$, $B = 7.6 \times 10^{-4}$, and $E = 1.4$. For R_{seal} we had no specific model and fit the data to $R_{seal} = 12.2C^{-0.29}$ primarily as a visual guide. Resistances were measured with a 20-mV test pulse, and all seals were made with 10-μm insertion into Sylgard. Each data point represents the mean of four or more seals with the same pipette. (*D*) Bi-ionic (Li^+/K^+) potentials as a function of concentration for the seals shown in *C*. The lines connect the mean of the data at each concentration. The voltages are pipette potentials and have not been corrected for junction potentials.

solution mobility, implying substantial interaction between the ions and the interior of the channel. The anion/cation permeability of rubber channels (Table 1) was higher than that of nicotinic channels where Dwyer et al. (1980) estimated the maximum P_{Na^+}/P_{Cl^-} to be 0.01. As Dywer et al. point out, however, it is difficult to rule out the possibility of anions altering the cation permeability.

We examined bi-ionic potentials as a function of concentration for one pair of ions, Li^+ and K^+, looking for evidence of concentration-dependent permeabilities (Dani, 1989). The difficulty with this kind of experiment (as with the dilution experiments) was that we could not use the same pipette for all the measurements, with the result that there was pronounced scatter in the data. Figs. 3, *C* and *D*, show data from a bi-ionic experiment of LiCl versus KCl across four orders of magnitude in concentration. Each data point represents the mean of a series of four or more seals with a single pipette (the standard errors are generally less than the symbol size). The variation of pipette resistance with concentration could not be fit with the Debye-Huckel-Onsager (DHO) conductance equation (Dani, 1989) but required a more complicated model containing a DHO volume conductor in parallel with a surface (double layer) conductor whose conductance varied as the square root of concentration (Davies and Rideal, 1963). The seal resistance varied more slowly with concentration than did the pipette resistance, but it did not saturate. The bi-ionic potentials varied in a nonmonotonic way with concentration (Fig. 3 *D*) suggesting multiple binding sites in the pathway. The nonmonotonic selectivity at high concentrations might also be influenced by the osmotic pressure exerted by the exclusion of Cl^- from the pathway (see below).

In addition to the DC measurements of reversal potentials, we made recordings of the current-voltage (I/V) curves (Figs. 4, *A* and *B*). In only a few cases could the data be fitted by the GHK equation with constant coefficients. We also tried fitting the data to symmetrical two-barrier one-site models, but these also did not fit in most cases, because the observed I/V data did not increase exponentially at high voltages. We made no attempt to fit more elaborate barrier models.

Since the cation and anion permeabilities of the channels are different, they should produce streaming potentials (Levitt et al., 1978; Rosenberg and Finkelstein, 1978; Dani, 1989). We tested this by using symmetrical solutions in the pipette and bath and then perfused the bath side of the seal with the same solution with sucrose added as an osmolyte to induce water flow (Dani, 1989). The streaming potential (V_s) was negative, and its magnitude increased linearly with osmotic pressure (Fig. 5). Unstirred layers (Levitt et al.,1978; Rosenberg and Finkelstein, 1978; Dani, 1989) did not seem

TABLE 1 Dilution potentials

Salt	Gradient	V_r (mV)	SE	N	P_X/P_{Cl^-}
NaCl	400:40	−55.5	2.5	15	90.7
KCl	400:40	−54.5	1.3	15	63.3
CsCl	400:40	−53.7	4.4	15	51.1
RbCl	400:40	−52.3	1.1	15	37.6
LiCl	400:40	−51.5	2.4	20	33.0
Guan.Cl	400:40	−49.3	2.0	20	23.4
HCl	400:40	−47.6	4.0	15	18.9
$MgCl_2$	200:20	−23.0	0.8	20	10.9
$SrCl_2$	200:20	−18.7	6.2	24	5.5
$CaCl_2$	200:20	−18.4	1.0	20	5.3
TrisCl	400:40	−24.2	13.3	22	3.4
$BaCl_2$	200:20	−9.3	1.2	21	2.1
$MnCl_2$	200:20	3.5	7.4	25	0.8
Arg.Cl	400:40	9.2	3.9	21	0.6
$LaCl_3$	133:13	25.7	3.0	25	0.1
AChCl	400:40	37.9	8.6	25	0.1

Dilution potentials obtained with borosilicate pipettes inserted 10.5 μm into a Sylgard surface. V_r, has been corrected for liquid junction potentials. Errors are standard errors of the mean for three or more pipettes with repeated seals and the number in parenthesis is the total number of measurements. P_X/P_{Cl^-} was calculated from the GHK equation. Data was obtained from seals without obvious gating transitions. Abbreviations: Arg = arginine, ACh = acetylcholine; Guan = guanidine, Tris = trihydroxymethylaminomethane.

TABLE 2 Cation selectivity from bi-ionic potentials

Salt	V_r (mV)	SE	N	P_X/P_{Na^+}
H^+	42.44	1.88	9.00	5.53
Cs^+	38.01	0.60	8.00	4.64
Rb^+	36.06	1.34	8.00	4.29
K^+	30.11	0.70	8.00	3.38
$Guan^+$	6.12	0.81	9.00	1.28
Na^+				1.00
Li^+	−30.91	0.83	8.00	0.27
Arg^+	−31.53	4.82	11.00	0.26
Ca^{2+}	−50.08	1.33	11.00	0.06
Ba^{2+}	−51.17	0.87	10.00	0.06
Sr^{2+}	−55.05	1.75	9.00	0.04
Mn^{2+}	−66.20	1.06	12.00	0.02
$Tris^+$	−74.22	2.21	10.00	0.02
Mg^{2+}	−69.30	2.50	11.50	0.02
				P_X/P_{Tris}
Li^+	11.50	1.02	15.00	2.41
ACh^+	4.38	0.92	29.00	1.41
Arg^+	0.08	1.86	35.00	1.01
$Tris^+$				1.00
Ca^{2+}	−13.53	0.40	15.00	0.30
				$P_X/P_{Mg^{2+}}$
Ca^{2+}	2.03	0.00	12.00	1.19
Mg^{2+}				1.00
Ba^{2+}	−0.01	0.07	12.00	1.00
Sr^{2+}	−1.10	0.00	12.00	0.91
Mn^{2+}	−3.80	0.00	12.00	0.72

Cation selectivity of seals obtained with borosilicate pipettes pressed into Sylgard surfaces under biionic conditions. For the upper table, the pipette contained 400 mM NaCl and the bath contained the indicated salts with Cl^- held at 400 mM. The permeability ratio of the ions relative to Na^+, P_X/P_{Na^+}, was computed from the GHK equation with allowance for a finite Cl^- permeability ($P_{Na^+}/P_{Cl^+} = 90.7$, Table I). The middle table used 400 mM TrisCl as the reference solution and the bottom table used 200 mM $MgCl_2$ as the reference. V_r has been corrected for liquid junction potentials. The data is the average from three reference pipettes exposed to the complete range of indicated ions with three or more seals per pipette at each condition. Because we measured potentials on a digital meter with only 1 mV resolution, the most stable potentials gave errors of 0.

to be a problem in these experiments as evidenced by the lack of "creep" in the potentials. (As opposed to the experiments on bilayers where diffusion occurred in one dimension, in our experiments diffusion occurred in three dimensions and consequently much faster. Also, our rapid local perfusion further reduced diffusional gradients). As expected from the nicotinic channel (Dani, 1989), the more permeant ions had smaller streaming potentials than did the less permeant ions (Fig. 5). Presumably this occurs because the more permeant ions are smaller and permit more water to pass between themselves and the channel walls. For K^+, the mean value of V_s was 1.93 ± 0.17 (N = 5) mV/Osm and for $Tris^+$, 2.55 ± 0.29 (N = 15) mV/Osm, corresponding to a respective coupling of N_{H_2O} = 1.2 and 4.2 molecules of water per ion. For large cations in the nicotinic ACh channel, N_{H_2O} = 3–4 (Dani, 1989) and in gramicidin 6–12 (Levitt et al.1978; Rosenberg and Finkelstein, 1978).

From dilution potentials (Table 1), $P_{Tris^+}/P_{Cl^-} \cong 3$ so we were surprised at the magnitude of V_s since we expected significant flux coupling of both $Tris^+$ and Cl^- with a commensurate lowering of V_s. We repeated the dilution potentials in the presence of 1 M sucrose and found that P_{Tris^+}/P_{Cl^-} increased by about 7-fold. We think that the osmotic pressure of 27 atm/Osm of a 1 M sucrose solution probably compressed the channel thereby increasing its selectivity. Similar alterations might occur during measurements on biological channels so that the measured properties may not necessarily reflect the properties of the unstressed channel. Assuming that $Tris^+$ spans the pore and that the Cl^- flux may be ignored, the above data place a lower limit on the length of the narrowest portion of the channel. From space-filling models, the mean diameter of $Tris^+$ is ≅7.5 Å. A cylinder that diameter would have to be ≅7 Å long to hold the four water molecules coupled to each $Tris^+$ ion. Apparently the multiple ion binding sites suggested by the concentration dependence of the bi-ionic potentials (Fig. 3 *D*) are close together.

DISCUSSION

We believe that the ionic pathway of the seal is between the substrate and the pipette rather than through the walls of the pipette or through the substrate. As a test, we made thick wall tips to reduce the effect of volume conduction through the glass. Tips were thickened by fire polishing with, respectively, a gas flame for quartz or a hot wire for glass. By changing the puller settings, we also made tips of variable diameter and wall thickness (OD 0.6–2.4 mm, ID 0.3–1.7 mm). The basic permeability properties of the seal were unaffected by wall thickness. When we sealed pipettes shut by fire polishing, the resistances were unmeasurably high. Surprisingly, treating the glass pipettes with methylating silane also did not change the cationic selectivity of the seal.

Since silanized glass, quartz, and Sylgard have negligible surface charge (Corey and Stevens, 1983), we presume the selectivity arises from dipolar fields, most likely the Si-O

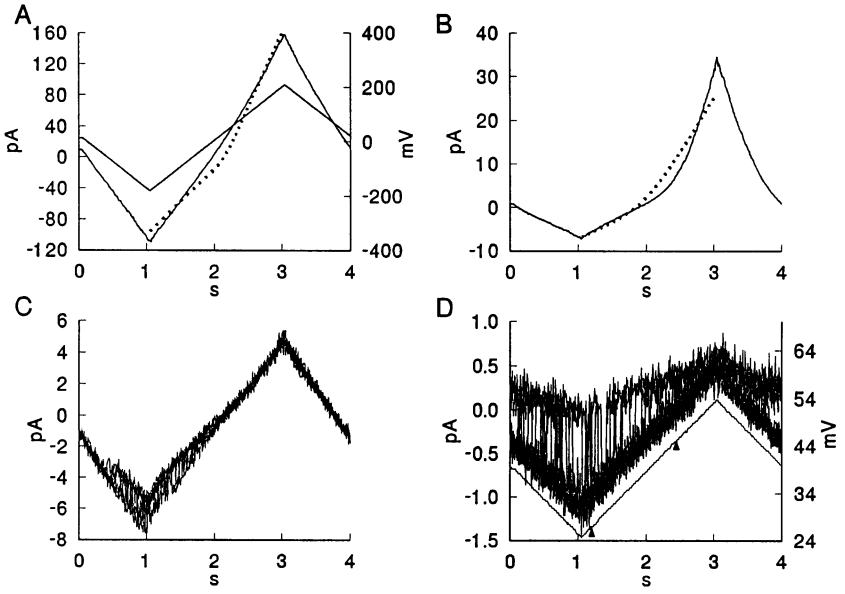

FIGURE 4 Current-voltage properties of seals using ramp voltage stimuli. (*A*) Nearly linear *I/V* curve with 100:1 concentration gradient, pipette 2 mM $CaCl_2$, bath 200 mM $CaCl_2$. DC measurements gave a corrected reversal potential of 22 mV showing cation selectivity. The dotted line is the best fit to the GHK equation with $P_{Ca^{2+}} = 2.4 \times 10^{-16}$ cm^3/s and $P_{Cl^-} = 2.2 \times 10^{-16}$ cm^3/s. (*B*) Na^+ is more permeable than arginine and current increases super linearly with voltage suggesting a rate limiting barrier to permeation. Pipette: 400 mM NaCl, bath: 400 mM arginine. Voltage stimulus as in *A*. Fit to the GHK equation for the region from −200 to +200 mV with the three permeabilities ($\times 10^{16}$ cm^3/s) as free parameters is shown by the dotted line; $P_{Arg^+} = 0.03$, $P_{Na^+} = 0.13$, $P_{Cl^-} = 0.002$. (*C*) Channel gating can depend on voltage and ion species. Pipette 40 mM LiCl, bath 40 mM KCl. Voltage was as in *A*. With negative potentials, i.e., K^+ being drawn from the bath into pipette, the channel is more likely to be in the low conductance state. Overlap of eight separate traces. (*D*) Different selectivity of high and low conductance states. The lower trace is the voltage stimulus (*right axis*). The noisy upper traces (*16 superimposed*) are current records from a spontaneously gating channel (*left axis*). The upper triangular envelope comes from the low conductance (12 pS) state, while the lower envelope comes from the high conductance (44 pS) state, and the vertical connecting lines represent state transitions. The reversal potentials of each state are indicated by the two arrows, 25 mV for the low conductance state and 45 mV for the high conductance state. Correcting for the liquid junction potential gives a net reversal potential of −9 mV for the low conductance state and +11 mV for the high conductance state. The pipette contained 2 mM $CaCl_2$, and the bath contained 200 mM $CaCl_2$.

bonds (Corey and Stevens, 1983) which, based on the channel's selectivity for cations, must lie with the oxygens closer to the interface. The conducting pathway of a seal, we believe, consists of thin strands of water snaking through the interface. A suggestive model can be made by putting a drop of water between two hydrophobic microscope slides. Pressing on the slides together produces a fractal array of water fingers whose shapes change when the slides are squeezed. The force between a pipette and Sylgard extrudes water from the interface. This dehydration is also favored by image forces arising from the low dielectric constants (4–6) of Sylgard and the pipette. Opposing the dehydration is the osmotic pressure of water (≅1300 atm) and whatever hydrophilic interactions are present on the glass. We presume that thermal fluctuations in the balance of these large forces lead to pinching off one or more pathways thereby gating the seal and producing channel like activity. It is not clear how increases in voltage can cause channel closure. One might imagine that breaking a conducting path would leave a high potential across the separated ends which would tend to accelerate reconstitution of the pathway, but this was not observed.

Regardless of the details, these data suggest that discrete gating does not require elaborate molecular structures, such as exist in biological channels, and that biological channel gating could involve hydrophobic residues in the permeation pathway. The pipette/Sylgard interfacial pathway has one hydrophobic wall but yet conducts ions at rates similar to membrane bound channels. This suggests that channels may not require a hydrophilic lining to support high rates of permeation. The kind of selectivity and gating observed here might occur in apparently undifferentiated ionic pathways such as epithelial tight junctions (Gilula, 1974) where, although the surfaces are not likely to be hydrophobic, water can be trapped in a thin layer between two membranes.

Water confined in narrow spaces has been predicted to form ordered structures consisting of rings or nets of water molecules (Edmonds, 1984). These calculations showed that the ordered water array can provide a multitude of low energy binding sites for ions and these sites are selective for the crystal radius, valence and sign of the ionic charge. Ions find low energy sites at the centers of the water rings and move through the structure by passing from water ring to contiguous water ring. These rings may also undergo a cooperative conformational change (that could appear as gating) either spontaneously or by being driven with an external electric field. Recently, Lev et al. (1993) showed that nanometer-sized pores in a hydrophobic membrane supported in a bilayer chamber can produce gated ionic currents.

What is the relevance of these data for membrane patch clamping? Possibly nothing, since the properties of

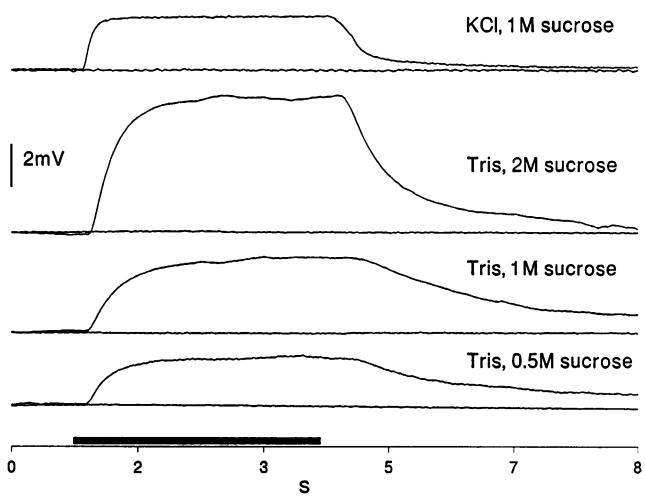

FIGURE 5 Streaming potentials for borosilicate pipettes inserted 10 μm into Sylgard surfaces, with negative potentials upward. Pipettes and the bath were filled with either 400 mM KCl or TrisCl, and the seal was perfused for the period shown by the black bar above the abscissa with the same solution plus the osmoticant shown at the right of the trace. The baseline of each trace was made as above, but with the pipette was lifted just over the surface.

Sylgard are very different from those of membranes. However, the cationic selectivity observed for all the materials involved suggests that details of the interaction may not be important. We re-examined the data of Fischmeister et al (1986) for heart cell patches (their Fig. 4). With 91 mM $CaCl_2$ in the pipette and 142 mM NaCl in the bath, the reversal potential of the seal was 24 mV, after making corrections for the liquid junction potential. From the GHK equation, $P_{Na^+}/P_{Ca^{2+}} > 4.8$. Their *I/V* curve showed the expected rectification. (The data of Fischmeister et al. (1986) did not show channel-like activity nor was mention made of any such observation.) By comparison, for rubber channels $P_{Na^+}/P_{Ca^{2+}} \cong 16$ (Table 2).

Background currents do not generally affect typical single channel measurements, since the baseline is operationally defined as the current adjacent to an opening. However, if one tries to measure the properties of a low conductance (nominally closed) state, or of pump and carrier currents where discrete transitions are not visible, proper allowance for background currents is essential. Our data and Fishmeister et al.'s (1986) data suggest that changing bath solutions on a formed patch will change the background current.

If gated channels can arise in the seal region of a membrane patch, there is a potential for misinterpreting data. When the channel under study can be gated by physiologically relevant stimuli, there is little confusion, but when channel activity is recorded from unfamiliar preparations and the relevant modulators are unknown, caution is necessary.

We would like to thank Guido Zamphigi for helpful discussions. This work was supported by the Medical Research Council and a Fogarty Fellowship (to F. Sachs) and Sutter Instruments. We would like to thank Dr. Denis Noble for pointing out Edmonds' work.

A preliminary account of this work in abstract form has been published (Sachs, F., and Q. Feng. 1993. Gated, ion-selective channels observed without membranes: novel properties of the gigaseal. *J. Physiol.* 128P).

REFERENCES

Adams, D. J., T. M. Dwyer, and B. Hille. 1980. The permeability of endplate channels to monovalent and divalent metal cations. *J. Gen. Physiol.* 75: 493–510.

Adams, D. J., W. Nonner, T. M. Dwyer, and B. Hille. 1981. Block of endplate channels by permeant cations in frog skeletal muscle. *J. Gen. Physiol.* 78:593–615.

Corey, D. P, and C. F. Stevens. 1983. Science and technology of patch recording electrodes. *In* Single Channel Recording. B. Sakmann, and E. Neher, editors. Plenum Publishing Corp., New York. 53–68.

Dani, J. A. 1989. Open channel structure and ion binding sites of the nicotinic acetylcholine receptor channel. *J. Neurosci.* 9:884–892.

Davies, J. T., and E. K. Rideal. 1963. Interfacial Phenomena. Academic Press, London.

Dwyer, T. M., D. J. Adams, and B. Hille. 1980. The permeability of the endplate channel to organic cations in frog muscle. *J. Gen. Physiol.* 75: 469–492.

Edmonds, D. T. 1984. Ordered water model of membrane ion channels. *In* Biological Membranes. D. Chapman, editor. Academic Press, London. 349–386.

Fischmeister, R., R. K. Ayer, and R. L. DeHann. 1986. Some limitations of the cell-attached patch clamp technique: a two electrode analysis. *Pfluegers Arch. Eur. J. Physiol.* 406:73–82.

Gilula, N. 1974. Junctions between cells. *In* Cell Communication. R. P. Cox, editor. John Wiley & Sons, New York. 1–29.

Hille, B. 1984. Ionic channels of excitable membranes. Sinauer Associates, Sunderland, MA.

Lev, A. A., Y. E. Korchev, T. K. Rostovtseva, C. L. Bashford, D. T. Edmonds, and C. A. Pasternak. 1993. Rapid switching of ion current in narrow pores: implications for biological ion channels. *Proc. R. Soc.* B252:187–192.

Levitt, D. G., S. R. Elias, and J. M. Hautman. 1978. Number of water molecules coupled to the transport of sodium, potassium and hydrogen ions via gramicidin, nonactin or valinomycin. *Biochim. Biophys. Acta.* 512:436–451.

Rosenberg, P. A., and A. Finkelstein. 1978. Interaction of ions and water in gramicidin A channels. *J. Gen. Physiol.* 72:327–340.